

Trade Science Inc.

Research & Reviews In

Electrochemistry

Full Paper

RREC, 2(1), 2010 [50-59]

Synergistic effect of chloride and bromide ions on corrosion inhibition of steel in 1 mol L⁻¹ phosphoric acid using cationic gemini surfactant

Zhen-Yu Wu^{1,2}, Zheng Fang¹, Wang Zhang², Ling-Guang Qiu^{2*}, An-Jian Xie², Yu-Hua Shen²¹School of Chemistry and Chemical Engineering, Central South University, Changsha 410083, (CHINA)²Laboratory of Advanced Porous Materials, School of Chemistry and Chemical Engineering, Anhui University, Hefei 230039, (CHINA)

E-mail : lgqiu@ahu.edu.cn

Received: 1st March, 2010 ; Accepted: 11th March, 2010

ABSTRACT

Synergism between a cationic gemini surfactant, 1,2-ethane-bis(dimethyl dodecyl ammonium bromide) (12-2-12), and halide ion (Br⁻ or Cl⁻) for corrosion inhibition of cold rolled steel in 1.0 mol L⁻¹ phosphoric acid was investigated by using weight loss, potentiodynamic polarization and electrochemical impedance spectroscopy (EIS) methods. Some thermodynamic parameters were calculated by fitting experimental data with Langmuir model. Potentiodynamic polarization studies reveal that the inhibition species is a mixed-type inhibitor. EIS measurements suggest that the presence of inhibitor molecules in acidic solution decreases double layer capacitance and increases the charge transfer resistance, indicating the formation of a protective layer on steel surface.

© 2010 Trade Science Inc. - INDIA

KEYWORDS

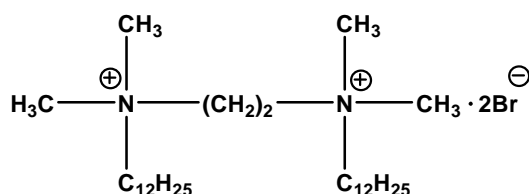
Gemini surfactants;
Corrosion inhibition;
Synergetic effect;
Steel;
Electrochemical.

INTRODUCTION

Acid solutions are widely used in industry, and in many cases corrosion inhibitors are used to prevent metal corrosion in acidic solution^[1-3]. Commonly, enough inhibitor needs to be used for corrosion inhibition of metal, for many inhibitors that are used in low concentrations bring about pitting corrosion, and using too small an amount of an inhibitor may be much worse than not using any inhibitor at all^[2-10]. For this reason, inhibitors are used in higher concentrations to avoid pitting corrosion. In recent years, synergistic effect on corrosion inhibition of metal have been widely investigated in different corrosive media, and it has been

clearly demonstrated that synergism between the corrosion inhibitor and another chemical substance is an effective means to improve the performance of inhibitors and reduce the cost for corrosion protection of metal^[5-23].

It is known that halide ions show a synergistic effect with many organic inhibitors, such as cyclohexylamine, propargyl alcohol, polyacrylamide (PA), gum arabic (GA) and polyethylene glycol (PEG), methionine, and indigo dye, on corrosion inhibition of steel, iron and its alloys in acidic media^[2,24-34]. Synergistic effect between halide ions and quaternary ammonium type surfactants on corrosion inhibition of steel in acid solution has also been investigated^[35-37]. The results demonstrate that the



Scheme 1 : Molecular structure of the gemini surfactant 12-2-12

addition of halide anions to corrosive medium can significantly improve performance of quaternary ammonium salt-type surfactant for corrosion inhibition of steel, which is attributed to the synergistic effect between halide anions and positive quaternary ammonium ions present in the inhibitor molecule. This is because the steel surface is positively charged in acidic solutions at the corrosion potential but becomes negatively charged when halide anions are present. Although a number of studies on synergistic inhibition between halide ion and some compounds for steel corrosion in H_2SO_4 have been reported, only a few investigations focus on synergism between halide ion and organic inhibitors for corrosion inhibition of steel in H_3PO_4 [38-41].

Gemini surfactant is a new generation surfactant developed in recent years. Differing from conventional single-chained surfactants, gemini surfactants consist of two hydrophilic head groups, two hydrophobic chains, and a spacer linked at or near the head groups. It has been demonstrated by our group [42-47] and some other researchers [48-51] that some cationic gemini surfactants, such as alkanediyl- α,ω -bis-(dimethylalkyl-ammonium bromide) series, are excellent candidates for iron and steel in acidic media. However, high cost of gemini surfactant retards their practical applications in corrosion inhibition of metal. Very recently, we investigated synergistic effect between cationic gemini surfactants and halide ions to corrosion protection of cold rolled steel in sulphuric acid solution by using weight loss [43] and electrochemical methods [44], and attempted to clarify mechanism of synergistic effect between gemini surfactants and halide ions. The results reveal that halide ions are effective additives for cationic gemini surfactant in corrosion inhibition system of steel in 0.5 mol L^{-1} H_2SO_4 . This novel composite inhibitor system was found to be efficient and low-cost for steel corrosion inhibition in sulphuric acid, even when concentration of the gemini surfactant used was as low as $1 \times 10^{-6} \text{ mol L}^{-1}$.

The purpose of this work is to study the synergistic inhibition between a cationic gemini surfactant, 1,2-ethane-bis(dimethyl dodecyl ammonium bromide) (designated as 12-2-12, Scheme 1), and halide ions (Br^- , or Cl^-) for steel corrosion in phosphoric acid, attempting to have a better understanding and get some general ideas to guide the composing of novel inhibitor system by halide ions and cationic gemini surfactants for corrosion protection of steel in acid solution.

EXPERIMENTAL

Potassium bromide, potassium chloride, sodium bromide, sodium chloride, and phosphoric acid were purchased from Shanghai Chemical Reagent Co. Ltd. (Shanghai, China). Double distilled water was used for preparing test solutions for all measurements. Cold rolled steel sample with composition $\text{C} \leq 0.1\%$, $\text{Mn} \leq 0.50\%$, $\text{P} \leq 0.035\%$, $\text{S} \leq 0.025\%$ and the remainder Fe was obtained from Cold Rolled Mill Plant of Baosteel (Shanghai, China). Gemini surfactant 12-2-12 was prepared and characterized by our laboratory as described previously and its critical micelle concentration (CMC) was determined to be $5.7 \times 10^{-4} \text{ mol L}^{-1}$ by using surface tension method and [44,45] and $8.92 \times 10^{-4} \text{ mol L}^{-1}$ by conductance method [46].

The weight loss experiment was carried out for 4 h at a desired temperature as reported previously [43-47]. All the tests were repeated three times in the experiment, with an average relative standard deviation less than 4 % in all cases. The corrosion rate of steel (r_{corr}) was calculated by the relation,

$$r_{\text{corr}} = (m_1 - m_2) / S \cdot t \quad (1)$$

where m_1 and m_2 are the mass of the specimen before and after corrosion, respectively, S the area of the specimen, and t the corrosion time.

Polarization and EIS measurements were carried out in a conventional three-electrode cell on a CHI604C Electrochemical Work Station (CH Instruments, Inc., Shanghai, China) with a platinum counter electrode (CE), a saturated calomel electrode (SCE) as the reference electrode, and a working electrode made of circle specimen of steel with a diameter of 0.85cm. The steel specimen was embedded in epoxy resin (Bison®, Holland), leaving its cross-section only. The electrode was ground on a series of emery papers down to 5000

Full Paper

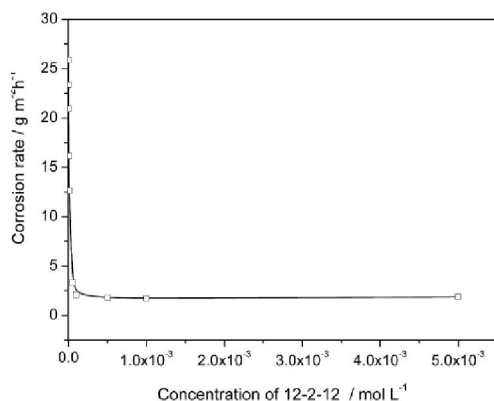


Figure 1 : Variation of the corrosion rate of cold rolled steel with concentration of 12-2-12 in 1.0 mol L⁻¹ phosphoric acid at 30C

grit (991A, MATADOR®, Germany), washed thoroughly with distilled water and acetone by ultrasonic, and dried in the air. Subsequently, the electrode was immersed in test solution for 0.5 h and then allowed to reach a comparatively stable open-circuit potential (OCP). The potentiodynamic current potential curves were recorded by automatically changing the electrode potential from potential of approximately +150mV to -150mV vs. corrosion potential (E_{corr}) at a scanning rate of 5mV s^{-1} . The frequency range for EIS used was from 100KHz to 0.05Hz. The amplitude of the applied sinusoidal signal was 10mV at initialization E (initialization E was given refer to E_{corr} come from potentiodynamic polarization curve and OCP). Resistances and capacitances were determined by fitting the EIS data with an equivalent circuit. All potentials were measured with respect to the SCE and all electrochemical experiments were carried out in aerated solutions at a temperature of $(30 \pm 0.02)^\circ\text{C}$.

RESULTS AND DISCUSSION

Weight loss method

Effect of 12-2-12 on corrosion rate of steel at 30°C

Although the main task of the present work is to investigate synergism between 12-2-12 and halide anions, before the synergism study corrosion inhibition of cold rolled steel by single 12-2-12 at various concentrations in 1.0 mol L⁻¹ phosphoric acid were studied to know the lowest concentration of 12-2-12 where a satisfied inhibition efficiency was obtained. Corrosion rates of cold rolled steel in the presence of

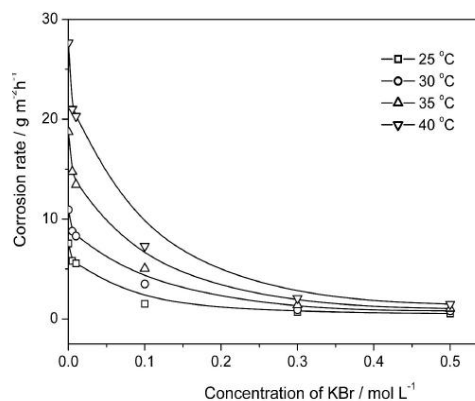


Figure 2 : Variation of the corrosion rate with KBr concentration in the presence of 1×10^{-5} mol L⁻¹ 12-2-12 at different temperatures

12-2-12 in various concentrations in 1.0 mol L⁻¹ phosphoric acid were determined at 30C, and the plot of corrosion rate of cold rolled steel vs. concentrations of 12-2-12 in 1.0 mol L⁻¹ phosphoric acid at 30°C is shown in figure 1. The results show that the corrosion rate decreases sharply with an increase in surfactant concentration when the surfactant concentration is lower than 5.0×10^{-4} mol L⁻¹. Further increase in surfactant concentration does not significantly reduce corrosion rate, suggesting saturated adsorption of surfactant molecules on steel surface. This result is similar to our previous study on corrosion inhibition of carbon steel in 1 mol L⁻¹ hydrochloric acid by the gemini surfactants 12-s-12 (s=2, 3, and 6)^[45]. Although 12-2-12 exhibited a high efficiency for corrosion inhibition of cold rolled steel in 1 mol L⁻¹ hydrochloric acid, higher concentration of the surfactant 12-2-12 used (up to 5.0×10^{-4} mol L⁻¹) leads to a high cost for its practical application. To reduce usage of the gemini surfactant 12-2-12, we attempted to introduce NaCl or KBr into the inhibitor system containing 12-2-12 at a lower concentration. It should be noted that only one temperature (30°C) was studied for corrosion inhibition of cold rolled steel in 1.0 mol L⁻¹ phosphoric acid by using 12-2-12, because this experiment was carried out just to decide a suitable surfactant concentration, at which the inhibition efficiency (IE) is not very high, to demonstrate whether there exists significant synergistic effect when halide salts is added.

Effect of Cl⁻ or Br⁻ on corrosion rate of steel in the presence of 12-2-12

To understand effects of Cl⁻ or Br⁻ on the corrosion inhibition of steel in 1.0 mol L⁻¹ phosphoric

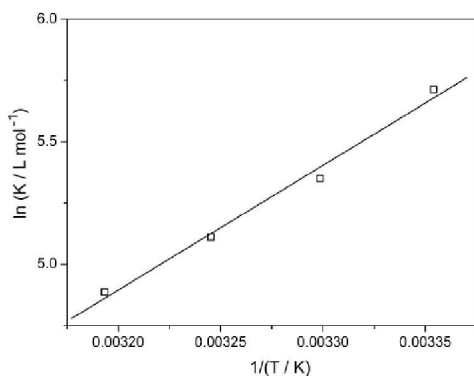


Figure 3 : Plots of $\ln K$ versus $1/T$ for 12-2-12/KBr system for corrosion inhibition of cold rolled steel in 1.0 mol L^{-1} phosphoric acid

acid in the presence of the gemini surfactant 12-2-12, dependence of corrosion rates on concentration of KBr or NaCl in the presence of surfactant 12-2-12 ($1 \times 10^{-5} \text{ mol L}^{-1}$, at which the inhibition efficiency was approximately 50% at 30°C) at $25\text{--}40^\circ\text{C}$ have been investigated. The results are shown in figure 2 and figure 1 (see Supplementary Material). It is clear that at a certain experimental temperature, corrosion rates of the specimen decrease sharply with increasing concentration of KBr or NaCl from 0.01 to 0.1 mol L^{-1} in the presence of $1 \times 10^{-5} \text{ mol L}^{-1}$ 12-2-12. Inhibition efficiency reaches to 90% when concentration of KBr or NaCl approaches to 0.1 M (12 g/L for KBr and 6 g/L for NaCl). At a certain concentration of KBr or NaCl, corrosion rates of specimen increase with an increase in corrosion temperature. However, further increase in salt concentration does not significantly decrease corrosion rate and increase the IE value (Figure 2 and Figure S1, Supplementary Material), which can be easily attributed to the saturated adsorption effect. This reveals that the addition of an inexpensive halide salt in gemini surfactant inhibitor system can largely reduce cost of the gemini surfactant for corrosion inhibition of steel in acidic medium. These results may be helpful for designing novel inhibitor system with high efficiency and low costs for corrosion inhibition of metal in corrosive media.

Adsorption isotherm for the complex of 12-2-12 and halide ions

Assuming the corrosion inhibition is caused by the adsorption of inhibitor molecules on steel surface, the degree of surface coverage (θ) for different concentrations of KBr or NaCl in 1.0 mol L^{-1} phosphoric acid

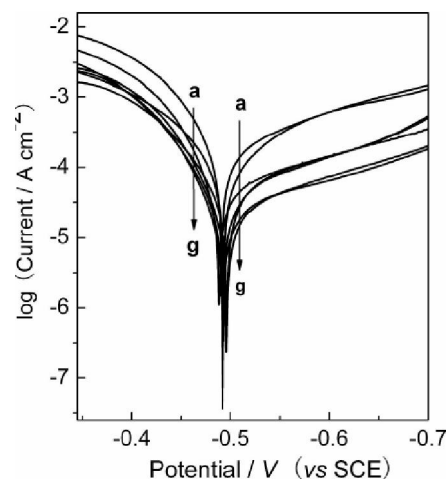


Figure 4 : Potentiodynamic polarization curves for 12-2-12 and 12-2-12/KBr systems in 1.0 mol L^{-1} phosphoric acid at 30°C . (a) Blank, (b) No KBr, (c)-(g) 0.005 , 0.01 , 0.1 , 0.3 , and 0.5 mol L^{-1} KBr, respectively. Inhibitor systems (b)-(g) also contain $1 \times 10^{-5} \text{ mol L}^{-1}$ 12-2-12

in the presence of $1 \times 10^{-5} \text{ mol L}^{-1}$ 12-2-12 can be evaluated from weight loss measurement using the Sekine and Hirakawa's method^[40]:

$$\theta = \frac{r_0 - r}{r_0 - r_m} \quad (2)$$

where r_0 and r are corrosion rates in the absence and presence of the inhibitor, respectively, and r_m the smallest corrosion rate.

Assuming the adsorption of inhibitor molecule on steel surface is monolayer adsorption, and lateral interactions between the inhibitor molecules is ignored, Langmuir adsorption isotherm can be applied to investigate the adsorption mechanism by the following equation^[52,53],

$$\frac{c}{\theta} = \frac{1}{K} + c \quad (3)$$

where K is the equilibrium constant of adsorption process and c the inhibitor concentration.

After calculating the surface coverage for 12-2-12/KBr or 12-2-12/NaCl system under different conditions, plot of c/θ versus KBr or NaCl concentration in the presence of $1 \times 10^{-5} \text{ mol L}^{-1}$ 12-2-12 at $25\text{--}40^\circ\text{C}$ are obtained (Figure S2 and S3). The linear regression between c/θ and c was done, and values of K and the corresponding parameters were estimated using Eq. (2) and (3), and the results are summarized in TABLE S1. It should be noted that only the linear regression between c/θ and c for 12-2-12 at

Full Paper

TABLE 1 : Thermodynamic parameters of 12-2-12/X (X = Br⁻ or Cl⁻) systems on steel surface in 1.0 mol L⁻¹ phosphoric acid at different temperatures

T	$\Delta G_{\text{ads}}^{\circ}$ (kJ mol ⁻¹)		$\Delta H_{\text{ads}}^{\circ}$ (kJ mol ⁻¹)		$\Delta S_{\text{ads}}^{\circ}$ (J mol ⁻¹ K ⁻¹)	
	12-2-12/KBr	12-2-12/NaCl	12-2-12/KBr	12-2-12/NaCl	12-2-12/KBr	12-2-12/NaCl
25°C	-24.12	-23.37	-42.31	-33.52	-61.02	-34.02
30°C	-23.61	-23.10	-42.31	-33.52	-61.71	-34.37
35°C	-23.38	-22.95	-42.31	-33.52	-61.43	-34.30
40°C	-23.18	-22.86	-42.31	-33.52	-61.10	-34.04

30°C was done by comparison. Both the linear correlation coefficients and slopes are close to 1, which means that the assumption is correct, i.e. the adsorption of 12-2-12 or 12-2-12/halide ion (Br⁻, or Cl⁻) on steel surface obeys the Langmuir adsorption isotherm. This result is also in accordance with our previous studies, in which adsorption of the gemini surfactants on the metal surface was found to conform to Langmuir adsorption model^[42-47].

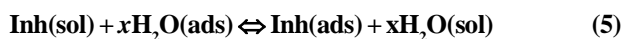
Thermodynamic parameters for the complex of 12-2-12 and halide ion

Thermodynamic model can be used to explain the adsorption phenomenon of inhibitor molecule. Using adsorption equilibrium constant (K) obtained by using Eq. (3), adsorption Gibbs free energy ($\Delta G_{\text{ads}}^{\circ}$), adsorption heat ($\Delta H_{\text{ads}}^{\circ}$) and adsorption entropy ($\Delta S_{\text{ads}}^{\circ}$) can be calculated. The adsorption heat could be calculated according to the Van't Hoff equation

$$\ln K = -\frac{\Delta H_{\text{ads}}^{\circ}}{RT} + \text{constant} \quad (4)$$

Plots of lnK versus 1/T for 12-2-12/NaCl and 12-2-12/KBr systems are shown in figure 3 and figure S4, respectively. It should be noted that ($\frac{\Delta H_{\text{ads}}^{\circ}}{R}$) is the slope of the straight line lnK versus 1/T according to Eq. (4), so the value of adsorption heat does not change with the unit of adsorptive equilibrium constant.

The adsorption of organic inhibitor molecules from the aqueous solution can be regarded as a quasi-substitution process between the inhibitor compound in the aqueous phase [Inh(sol)] and water molecules at the electrode surface^[25,36].



where x is the size ratio, that is, the number of water molecules replaced by one organic inhibitor. Thus, the standard adsorption Gibbs free energy could be

obtained according to

$$K = \frac{1}{C_{\text{solvent}}} \exp\left(\frac{-\Delta G_{\text{ads}}^{\circ}}{RT}\right) \quad (6)$$

where c_{solvent} is molar concentration of the solvent, which in the case of water is 55.5 mol L⁻¹. R is the universal gas constant, and T the absolute temperature (K).

Standard adsorption entropy can be calculated by using thermodynamic basic equation,

$$\Delta G_{\text{ads}}^{\circ} = \Delta H_{\text{ads}}^{\circ} - T\Delta S_{\text{ads}}^{\circ} \quad (7)$$

Thermodynamic parameters $\Delta G_{\text{ads}}^{\circ}$ and $\Delta S_{\text{ads}}^{\circ}$ at different temperatures, as well as $\Delta H_{\text{ads}}^{\circ}$ within the temperature region studied in this work were calculated using Eq. (4-7), and the results are listed in TABLE 1.

The values of thermodynamic parameters for the adsorption of inhibitors can provide valuable information about mechanism of adsorption of inhibitor molecules on metal surface. For example, an endothermic adsorption process ($\Delta H_{\text{ads}}^{\circ} > 0$) is attributed unequivocally to chemisorption^[37], while an exothermic adsorption process ($\Delta H_{\text{ads}}^{\circ} < 0$) may involve either physisorption or chemisorption or a mixture of both the processes. The negative values of $\Delta G_{\text{ads}}^{\circ}$ ensure the spontaneity of the adsorption process and stability of the adsorbed layer on the steel surface. $\Delta G_{\text{ads}}^{\circ}$ of single gemini 12-2-12 (-42.62 kJ mol⁻¹) calculated from Eq. (3) and (5) was found to be much more negative than values of 12-2-12/halide ion systems, which is consistent with our previous result^[43]. Generally, values of $\Delta G_{\text{ads}}^{\circ}$ around -20 kJ mol⁻¹ or higher are consistent with the electrostatic interaction between the charged molecules and the charged metal (physisorption); those around -40 kJ mol⁻¹ or lower involve charge sharing or transfer from organic molecules to the metal surface to form a coordinate type of bond (chemisorption)^[25,37]. Furthermore, $\Delta G_{\text{ads}}^{\circ}$ of 12-2-12/KBr is more negative than that of the 12-2-12/NaCl under the same condition, suggesting that adsorption of 12-2-12/Br inhibitor system on the steel surface is more stable than that of the 12-2-12/Cl system. In addition, the calculated values of the $\Delta H_{\text{ads}}^{\circ}$ for the adsorption of inhibitor molecules for 12-2-12/KBr and 12-2-12/NaCl inhibition systems are -33.52 and -42.31 kJ mol⁻¹, respectively. This result indicates that the adsorption is an exothermic process. The magnitude of adsorption heat is larger than the common physical adsorption heat, reaching the common chemical

TABLE 2 : Potentiodynamic polarization parameters for gemini surfactant 12-2-12 and 12-2-12/X⁻ (X⁻ = Br⁻ or Cl⁻) systems for corrosion inhibition of steel in 1.0 mol L⁻¹ phosphoric acid at 30°C

C _X ^[-a]	E _{corr} (V vs SCE)	-b _c (mV dec ⁻¹)	b _a (mV dec ⁻¹)	R _p (Ω cm ²)	I _{corr} (μA cm ⁻²)	E (%)
Blank	-0.491	239.6	64.7	57.33	385.85	/
0	-0.493	205.5	92.4	133.56	207.21	46.30
0.005 mol L ⁻¹ KBr	-0.488	251.0	49.5	172.88	103.85	73.08
0.01 mol L ⁻¹ KBr	-0.496	231.5	71.9	263.37	90.45	76.56
0.1 mol L ⁻¹ KBr	-0.492	209.4	60.8	451.30	45.33	88.25
0.3 mol L ⁻¹ KBr	-0.496	262.3	49.6	458.77	39.48	89.77
0.5 mol L ⁻¹ KBr	-0.492	233.0	50.6	513.59	35.19	90.88
0.005 mol L ⁻¹ NaCl	-0.497	224.7	81.3	207.61	124.86	67.64
0.01 mol L ⁻¹ NaCl	-0.486	306.6	56.5	213.74	96.92	74.88
0.1 mol L ⁻¹ NaCl	-0.497	269.3	47.8	281.67	62.58	83.71
0.3 mol L ⁻¹ NaCl	-0.495	255.5	61.3	462.75	46.39	87.98
0.5 mol L ⁻¹ NaCl	-0.493	227.5	50.8	467.39	38.58	90.00

^[a]All systems also contain 1×10⁻⁵ mol L⁻¹ 12-2-12 except the blank

adsorption heat. This probably means that the chemical adsorption also takes place besides physisorption. In addition, values of ΔS_{ads}° are negative, suggesting that a decrease in disordering takes places in going from reactants to the metal-adsorbed species reaction complex^[25,37].

Considering only electrostatic attraction effects, the adsorption of gemini surfactant molecules on metal surface is more complicated than that of conventional single-chained surfactants, because gemini surfactants contain two hydrophilic groups and two hydrophobic groups^[44-47]. It is unlikely that positive quaternary ammonium ions present in the inhibitor molecule will directly adsorb on the steel surface, because of electrostatic repulsion force among the quaternary ammonium cations gemini surfactant ions and the excess positive charge at the steel/acid solution interface at the corrosion potential^[28]. Halide ions have been proved to be effective additives as they increase the inhibiting tendency of positive quaternary ammonium ion by the well known synergistic effect^[28-31]. It is assumed that chloride or bromide ions first adsorb on the steel/solution interface through electrostatic attraction forces between these anions and the excess of positive charges at steel surface at the corrosion potential. This effect leads to a change on the solution side of the interface which becomes negatively charged. Thus, quaternary

TABLE 3 : Element values of equivalent circuit of EIS for gemini surfactant 12-2-12 and 12-2-12/X⁻ (X⁻ = Br⁻ or Cl⁻) systems on the steel surface in 1.0 mol L⁻¹ phosphoric acid at 30°C

C _X ^[-a]	OCF (V vs SCE)	E _{corr} (V vs SCE)	CPE (Y ₀ /μΩ ¹ S ⁿ cm ⁻²)	N (0-1)	R _s (Ω.cm ²)	R _{ct} (Ω.cm ²)	E (%)
Blank	-0.491	-0.491	649.26	0.8635	7.58	64.8	/
0	-0.482	-0.493	518.93	0.8321	4.78	135.2	52.09
0.005 mol L ⁻¹ KBr	-0.502	-0.488	301.03	0.7676	6.21	252.4	74.34
0.01 mol L ⁻¹ KBr	-0.486	-0.496	265.47	0.8455	5.46	306.8	78.89
0.1 mol L ⁻¹ KBr	-0.488	-0.492	248.77	0.8878	7.35	665.9	90.27
0.3 mol L ⁻¹ KBr	-0.498	-0.496	196.76	0.8266	8.83	1091.0	94.06
0.5 mol L ⁻¹ KBr	-0.478	-0.492	172.49	0.8856	9.68	1644.0	96.06
0.005 mol L ⁻¹ NaCl	-0.504	-0.497	307.12	0.8299	4.62	250.2	74.11
0.01 mol L ⁻¹ NaCl	-0.488	-0.486	263.31	0.8494	5.83	271.1	76.11
0.1 mol L ⁻¹ NaCl	-0.478	-0.497	228.71	0.8714	7.12	588.5	88.99
0.3 mol L ⁻¹ NaCl	-0.476	-0.495	203.56	0.8568	8.52	1069.0	93.94
0.5 mol L ⁻¹ NaCl	-0.487	-0.493	187.96	0.8758	7.69	1411.0	95.41

^[a]All systems also contain 1×10⁻⁵ mol L⁻¹ 12-2-12 except the blank

ammonium cations of the gemini surfactant are able to adsorb electrostatically on the steel surface previously covered with adsorbed chloride or bromine ions.

Electrochemical methods

Potentiodynamic polarization curves method

Potentiodynamic polarization curves of cold rolled steel in uninhibited and inhibited phosphoric acid solutions containing 12-2-12/KBr or 12-2-12/NaCl are shown in figure 4 and figure S5, respectively. Cathodic Tafel slopes (b_c) were calculated by Tafel extrapolation of the cathodic branches in the present work as shown in figure 5. However, accurate evaluation of the anodic Tafel slope (b_a) by Tafel extrapolation method is impossible, which is due to absence of linearity in the whole of the anodic branch. As a result, anodic Tafel slopes were calculated by using a modified Tafel extrapolation method^[54,55]. The cathodic Tafel region was first extrapolated to electrode potentials below the corrosion potential, and then the anodic current density i_a is calculated from^[54,55],

$$i_a (\text{net experimental}) = i_a - |i_c| \quad (8)$$

where |i_c| is the cathodic current density. Thus, the anodic current density is the sum of the experimentally observed anodic current density and the extrapolated cathodic current density. As a result, corrosion current density (i_{corr}), and anodic Tafel slope (b_a), as well as the polarization resistance R_p, for each inhibitor system were

Full Paper

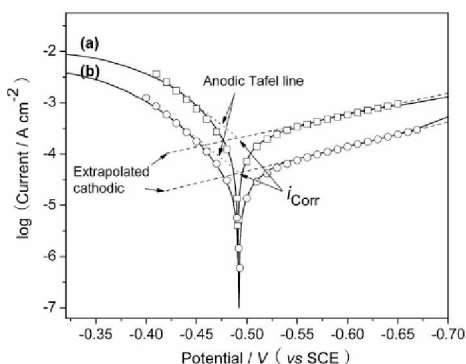


Figure 5 : Illustration of the determination of corrosion current and Tafel slopes from Tafel plots using the modified Tafel extrapolation method, and the calculated polarization curves for cold rolled steel without any inhibitor (\square) and in the presence of KBr/12-2-12 inhibitor system (\circ). Solid lines (a) and (b) represent experimental polarization curves for cold rolled steel without any inhibitor and in the presence of KBr/12-2-12 inhibitor system, respectively. $c_{\text{KBr}} = 0.1 \text{ mol L}^{-1}$, and $c_{12-2-12} = 1 \times 10^{-5} \text{ mol L}^{-1}$

estimated. Accordingly, the corrosion inhibition efficiency was evaluated from the measured i_{corr} values according to Eq. (9)^[56]. The results are summarized in TABLE 2. It is clear that both cathodic and anodic polarization branches calculated according to Eq. (10) and (11) fit well to the experimentally observed potentiodynamic polarization curves, as shown in figure 5.

$$E\% = \left(\frac{i_{\text{corr}} - i'_{\text{corr}}}{i_{\text{corr}}} \right) \times 100 \quad (9)$$

where i'_{corr} and i_{corr} are corrosion current densities with and without the addition of the inhibitor.

$$\log i_a = \log i_{\text{corr}} + \frac{E_i - E_{\text{corr}}}{b_a} \quad (10)$$

$$\log i_c = \log i_{\text{corr}} + \frac{E_{\text{corr}} - E_i}{b_c} \quad (11)$$

As can be seen from figure 4 and figure S5, the addition of 12-2-12/KBr or 12-2-12/NaCl system to 1.0 mol L^{-1} phosphoric acid leads to a decrease in both anodic and cathodic currents. This result reveals that both the 12-2-12/NaCl and 12-2-12/KBr inhibitor systems reduce cathodic hydrogen evolution reaction and also retard anodic metal dissolution. Furthermore, cathodic polarization branches give parallel Tafel lines with the nearly constant cathodic Tafel slopes. This result indicates that the addition of these inhibitors to the acid solution does not modify the proton reduction mechanism and this reaction is activation controlled. The inhibitor

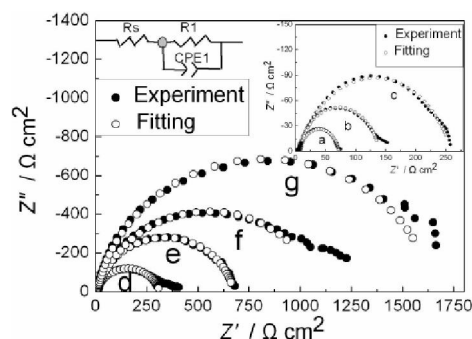


Figure 6 : Equivalent circuit for synergistic corrosion inhibition of steel in 1.0 mol L^{-1} phosphoric acid and Nyquist plots of experiment and fitting for 12-2-12 and 12-2-12/KBr systems with concentration of inhibitor at 30°C . (a) Blank, (b) No KBr, (c)-(g) 0.005, 0.01, 0.1, 0.3, and 0.5 mol L^{-1} KBr, respectively. Inhibitor systems (b)-(g) also contain $1 \times 10^{-5} \text{ mol L}^{-1}$ of 12-2-12

is first adsorbed on steel surface and therefore, impedes by merely blocking the active sites of steel surface. In this way, the surface area available for H^+ ions is decreased, while the actual reaction mechanism remains unaffected^[57]. In the anodic part of polarization curves, a significant inhibition was observed at low overpotentials, which may suggest formation of a protective layer of adsorbed species at the metal surface^[57]. However, inhibitor has little effect on the corrosion reaction at higher overpotential than -320mV , which is usually defined as desorption potential. This means that the inhibition mode of inhibitor depends on the electrode potential. The increasing current density at higher overpotentials may be the result of significant dissolution of metal, leading to desorption of inhibitor film from the metal surface^[57]. In addition, b_c and b_a values remain more or less identical in the absence and presence of inhibitors as shown in TABLE 2, indicating that the effect of inhibitors is not as large as to change the corrosion mechanism.

Electrochemical impedance spectroscopy (EIS) method

Typical sets of complex plane plots of mild steel in $1.0 \text{ mol L}^{-1} \text{ H}_3\text{PO}_4$ solution in the absence and presence of 12-2-12 and 12-2-12/halide ions inhibitor systems are shown in figure 6 and figure S6-S8, respectively. All plots have a depressed semicircular shape in the complex impedance plane with the centre under the real axis. This typical behaviour for solid metal electrodes shows frequency dispersion of the impedance data and

can be attributed to roughness and other inhomogeneities of the solid surface^[57,58]. In such cases, the parallel combination of double layer capacitance and charge transfer resistance which are in series with solution resistance ($(C_{dl}R_{ct})R_s$), particularly in the presence of an efficient inhibitor, is found to be an inadequate approach for modelling the interface. The use of the constant phase element (CPE) can be an effective way to represent the frequency dependence of nonideal capacitive behaviour, for example, corrosion of irregular and heterogeneous solid surfaces. The impedance of the CPE could be given by^[57]:

$$Z(\text{CPE}) = Y_0^{-1} (j\omega)^{-n} \quad (13)$$

where Y_0 is the magnitude of the CPE, j the imaginary unit, ω the angular frequency and n the phase shift which gives details about the degree of surface inhomogeneity.

To obtain accurate results the analysis of complex plane plots was done by fitting the experimental results with the equivalent circuit given in insert figure 6, which has been used previously to model the mild steel/acid interface^[58,59]. The circuit consists of solution resistance (R_s) in series with the parallel combination of charge transfer resistance (R_{ct}), and a constant phase element used in place of double layer capacitance (C_{dl}) to represent the nonideal capacitive behaviour of the double layer more clearly.

The inhibition efficiency was evaluated from the measured charge transfer resistance R_{ct} values as,

$$E\% = \frac{R_{ct}' - R_{ct}}{R_{ct}'} \times 100 \quad (14)$$

where R_{ct} and R_{ct}' are the charge transfer resistance values in the absence and presence of inhibitors.

As can be seen from figure 6, the calculated data based on equivalent circuit fit well to the experimental data, with an average relative standard deviation less than 4 % in all cases. The results obtained from these complex plane plots are also summarized in TABLE 3.

It is apparent that the charge transfer resistance value of cold rolled steel in uninhibited 1.0 mol L⁻¹ H₃PO₄ solution changes significantly after the addition of these inhibitors. The percent inhibition efficiencies of 12-2-12/NaCl mixture are slight lower than that of 12-2-12/KBr mixture. This result is somewhat expected because of as a rule inhibiting effect of halide ions in combination

with organic compounds in acidic medium increases in the order I⁻ > Br⁻ > Cl⁻.

It should be emphasized that high concentrations of NaBr also exhibit corrosion inhibition of cool rolled steel in 1.0 mol L⁻¹ phosphoric acid^[60], and ionic strength may influence corrosion inhibition of steel in acidic solution. However, by comparing the inhibition efficiency of single NaBr from the reference data and KBr/12-2-12 system at 30°C in the present work, one can easily find that IE of bromide salt in the presence of 12-2-12 is remarkably higher than that of single salt with the same concentration or only 1×10⁻⁵ mol L⁻¹ 12-2-12, especially when the salt concentration is lower than 0.1 mol L⁻¹ (TABLE S3). This result suggests 'apparent synergy' is mainly originated from a real synergism between the surfactant and the halide salt, rather than the halide anion itself or changes in ionic strength, though salt concentration and ionic strength may partially affect such the synergism at higher salt concentrations. Furthermore, by comparing values of adsorption Gibbs free energy ΔG_{ads}° for single NaBr and KBr/12-2-12 systems, one can find that the KBr/12-2-12 system has a more negative ΔG_{ads}° value. This result clearly suggests that the combination adsorption of 12-2-12 and halide anions leads to more stable adsorption of inhibitor molecules on steel surface, which is due to a synergetic inhibition effect.

Effects of cations of halide salts on corrosion inhibition of cold rolled steel

To have a better understanding of synergistic effects between halide salts and the gemini surfactant, and to clarify whether cations of these halide salts affect corrosion inhibition of cold rolled steel in 1.0 mol L⁻¹ H₃PO₄ solution in the presence of 1×10⁻⁵ mol L⁻¹ 12-2-12, control experiments were carried out by using another bromide and chloride salts, i.e. NaBr and KCl. Potentiodynamic polarizatin curves and EIS results are shown in figure S9-S12, and some electrochemical parameters obtained are summarized in TABLE 2. No effect of cations of the halide salts studied on inhibition efficiency was found in the present work, suggesting that synergism takes place just between cationic surfactant and halide anions. This can be easily explained in view of synergistic mechanism between surfactant cations and halide anion as discussed above.

Full Paper

CONCLUSIONS

Synergistic effect between the gemini surfactant and halide (bromide and chloride) ions on corrosion inhibition of cold rolled steel in 1.0 mol L⁻¹ phosphoric acid was studied using weight loss, potentiodynamic polarization and electrochemical impedance spectroscopy methods. The results suggest that 12-2-12/KBr or 12-2-12/NaCl inhibitor system acts as a mixed-type inhibitor for corrosion inhibition of cold rolled steel in phosphoric acid. It was found that 12-2-12/KBr and 12-2-12/NaCl synergistic inhibitor systems were efficient for steel corrosion in 1.0 mol L⁻¹ phosphoric acid. The adsorption mechanism of inhibitors was also investigated and the results reveal that the adsorption of inhibitor molecules on steel surface obeys the Langmuir adsorption model. Negative values of adsorption Gibbs free energy $\Delta G_{\text{ads}}^{\circ}$ and adsorption heat $\Delta H_{\text{ads}}^{\circ}$ for 12-2-12, 12-2-12/KBr, and 12-2-12/NaCl systems in 1.0 mol L⁻¹ phosphoric acid suggest that the adsorption of inhibitor molecules on steel surface is a spontaneous and exothermic process.

ACKNOWLEDGEMENTS

We are grateful for the financial supports from the Natural Science Foundation of China (20971001), Program for New Century Excellent Talents in University (NCET-08) from Ministry of Education, China, and the Key Project of Natural Science Foundation from Education Bureau of Anhui Province, China (kj2007A078).

REFERENCES

- [1] K.L.C.Babic-Samardzija, N.Hackerman, A.R.Barro; *J.Mater.Chem.*, **15**, 1908 (2005).
- [2] N.Calkan, S.Bilgic; *Appl.Surf.Sci.*, **153**,128 (2000).
- [3] M.Hosseinia, S.F.L.Mertensb, M.R.Arshadi; *Corros.Sci.*, **45**,1473 (2003).
- [4] H.Y.Ma, S.H.Chen, B.H.Yin, S.Y.Zhao, X.Q.Liu; *Corros.Sci.*, **45**, 867 (2003).
- [5] N.Ochoa, F.Moran, N.Perbere; *J.Appl.Electrochem.*, **34**, 487 (2004).
- [6] S.Rajendran, B.V.Apparao, N.Palaniswamy; *Electrochim.Acta*, **44**, 533 (1998).
- [7] H.Amar, J.Benzakour, A.Derja, D.Villemin, B.Moreau, T.Braisaz, A.Tounsi; *Corros.Sci.*, **50**, 124 (2008).
- [8] M.Forsyth, C.M.Forsyth, K.Wilson, T.Behrsing, G.B.Deacon; *Corros.Sci.*, **44**, 2651 (2002).
- [9] S.Rajendran, S.M.Reenkala, N.Anthony, R.Ramraj; *Corros.Sci.*, **44**, 2243 (2002).
- [10] T.A.Truc, P.Nadine, T.T.X.Hang, Y.Hervaud, B.Boutevin; *Corros.Sci.*, **44**, 2055 (2002).
- [11] K.Aramaki; *Corros.Sci.*, **44**, 871 (2002).
- [12] C.Georges, E.Rocca, P.Steinmetz; *Electrochim.Acta*, **53**, 4839 (2008).
- [13] H.A.El-Dahan, T.Y.Soror, R.M.El-Sherif; *Mater.Chem.Phys.*, **89**, 260 (2005).
- [14] E.E.Ebenso; *Mater.Chem.Phys.*, **79**, 58 (2003).
- [15] A.R.Yazdzad, T.Shahrabi, M.G.Hosseini; *Mater.Chem.Phys.*, **109**, 199 (2008).
- [16] **535**, 75 (2002).
- [17] R.F.V.Villamil, P.Corio, J.C.Rubim, S.M.L.Agostinho; *J.Electroanal.Chem.*, **472**, 112 (1999).
- [18] H.Tavakoli, T.Shahrabi, M.G.Hosseini; *Mater.Chem.Phys.*, **109**, 281 (2008).
- [19] M.G.Hosseini, H.Tavakoli, T.Shahrabi; *J.Appl.Electrochem.*, **38**, 1629 (2008).
- [20] K.Ramji, D.R.Cairns, S.Rajeswari; *Appl.Surf.Sci.*, **254**, 4483 (2008).
- [21] S.Sathiyarayanan, C.Jeyaprabha, G.Venkatachari; *Mater.Chem.Phys.*, **107**, 350 (2008).
- [22] C.Jeyaprabha, S.Sathiyarayanan, G.Venkatachari; *Appl.Surf.Sci.*, **253**, 432 (2006).
- [23] S.Y.Sayed, M.S.El-Deab, B.E.El-Anadouli; *J.Phys.Chem.B*, **107**, 5575 (2003).
- [24] Y.Feng, K.S.Siow, W.K.Teo, A.K.Hsieh; *Corros.Sci.*, **41**, 829 (1999).
- [25] S.A.Umoren, E.E.Ebenso; *Mater.Chem.Phys.*, **106**, 387 (2007).
- [26] S.A.Umoren, O.Ogbobe, I.O.Igwe, E.E.Ebenso; *Corros.Sci.*, **50**, 1998 (2008).
- [27] E.E.Oguzie, Y.Li, F.H.Wang; *Electrochim.Acta*, **52**, 6988 (2007).
- [28] E.E.Oguzie, Y.Li, F.H.Wang; *J.Colloid Interf .Sci.*, **310**, 90 (2007).
- [29] E.E.Oguzie, C.Unaegbu, C.N.Ogukwe, B.N.Okolue, A.I.Onuchukwu; *Mater.Chem.Phys.*, **84**, 363 (2004).
- [30] L.Larabi, Y.Harek, M.Traisnel, A.Mansri; *J.Appl.Electrochem.*, **34**, 833 (2004).
- [31] A.S.Fouda, H.A.Mostafa, F.El-Taib, G.Y.Elewady; *Corros.Sci.*, **47**, 1988 (2005).
- [32] M.Bouklah, B.Hammouti, A.Aouniti, M.Benkadour, A.Bouyanzer; *Appl.Surf.Sci.*, **252**, 6236 (2006).

- [33] C.Jeyaprabha, S.Sathiyarayanan, G.Venkatachari; *Electrochim.Acta*, **51**, 4080 (2006).
- [34] C.Jeyaprabha, S.Sathiyarayanan, G.Venkatachari; *J.Electroanal.Chem.*, **583**, 232 (2005).
- [35] Z.A.Chikh, D.Chebabe, A.Dermaj, N.Hajjaji, A.Srhiri, M.F.Montemor, M.G.S.Ferreira; *Corros.Sci.*, **47**, 447 (2005).
- [36] M.A.Deyab; *Corros.Sci.*, **49**, 2315 (2007).
- [37] B.Jabeera, S.M.A.Shibli, T.S.Anirudhan; *Appl.Surf.Sci.*, **252**, 3520 (2006).
- [38] L.B.Tang, X.M.Li, G.N.Mu, L.Li, G.H.Liu; *Appl.Surf.Sci.*, **253**, 2367 (2006).
- [39] X.M.Li, L.B.Tang; *Mater.Chem.Phys.*, **90**, 286 (2005).
- [40] G.N.Mu, X.M.Li, F.Li; *Mater.Chem.Phys.*, **86**, 59 (2004).
- [41] X.M.Li, L.B.Tang, H.C.Liu, G.N.Mu, G.H.Liu; *Mater.Lett.*, **62**, 2321 (2008).
- [42] L.G.Qiu, Y.Wu; 'Corrosion Inhibition of Steel in Acidic Medium by Cationic Gemini Surfactants', In: E.L.Bettini Eds., 'Progress in Corrosion Research', Nova Science Publishers, Inc., New York, 159-185 (2007).
- [43] L.G.Qiu, Y.Wu, Y.M.Wang, X.Jiang; *Corros.Sci.*, **50**, 576 (2008).
- [44] Z.Y.Wu, Z.Fang, L.G.Qiu, Y.Wu, Z.Q.Li, T.Xu, W.Wang, X.Jiang; *J.Appl.Electrochem.*, **39**, 779 (2009).
- [45] L.G.Qiu, A.J.Xie, Y.H.Shen; *Appl.Surf.Sci.*, **246**, 1 (2005).
- [46] L.G.Qiu, A.J.Xie, Y.H.Shen; *Mater.Chem.Phys.*, **91**, 269 (2005).
- [47] L.G.Qiu, A.J.Xie, Y.H.Shen; *Corros.Sci.*, **47**, 273 (2005).
- [48] Mel.Achouri, S.Kertit, H.M.Goultaya, B.Nciri, Y.Bensouda, L.Perez, M.R.Infante; *Prog.Org.Coat.*, **43**, 267 (2001).
- [49] Mel.Achouri, M.R.Infante, F.Izquierdo, S.Kertit, H.M.Goultaya, B.Nciri; *Corros.Sci.*, **43**, 19 (2001).
- [50] W.Huang, J.X.Zhao; *Colloids Surf.A*, **278**, 246 (2006).
- [51] S.Z.Yao, X.H.Jiang, L.M.Zhou, Y.J.Lv, X.Q.Hu; *Mater.Chem.Phys.*, **104**, 301 (2007).
- [52] M.L.Free; *Corros.Sci.*, **44**, 2865 (2002).
- [53] M.L.Free; *Corros.Sci.*, **46**, 3101 (2004).
- [54] E.McCafferty; *Corros.Sci.*, **47**, 3202 (2005).
- [55] K.F.Khaled, M.A.Amin; *Corros.Sci.*, **51**, 1964 (2009).
- [56] R.G.Kelly, J.R.Scully, D.W.Shoesmith, R.G.Buchheit; 'Electrochemical Techniques in Corrosion Science and Engineering', Marcel Dekker, Inc., New York, (2002).
- [57] R.Solmaz, G.Kardas, B.Yazici, M.Erbil; *Colloids Surf.A*, **312**, 7 (2008).
- [58] M.Ozcan, R.Solmaz, G.Kardas, I.Dehtri; *Colloids Surf.A*, **325**, 57 (2008).
- [59] A.Popova; *Corros.Sci.*, **49**, 2144 (2007).
- [60] L.B.Tang, X.M.Li, H.C.Liu, G.N.Mu; *J.Mater.Sci.*, **41**, 1991 (2006).